

## Reply to Anonymous Referee #1

→ Specific changes have been made in response to the reviewer's comments and are described below. The reviewer's comments are recalled in blue and changes in the revised version are highlighted in yellow.

### Summary

The authors used ground-based remote sensing observations collected during the summertime over the course of 4 years at a continental site in Antarctica to explore the change in net surface fluxes caused by the presence of supercooled liquid-phase clouds. The authors find a strong relation between condensate amount (i.e., liquid water path, LWP) to ambient temperature. By using a clear-sky reference (i.e., selected days that were cloud-free), the authors extract changes in the surface radiative fluxes as a function of LWP and predict an Antarctic-wide change in the surface net radiative budget. The article is well written and contains interesting analysis. As listed below, there are several major concerns that make it difficult to support the authors' conclusions. Since the article touches on a highly relevant topic, I recommend a resubmission of this paper after resolving all major concerns.

→ Thank you for your positive remarks in order to improve the quality of the manuscript. All your comments have been taken into account. An in-depth study has been performed to evaluate the choice of the clear-sky reference.

### Major concerns

My main concern is the choice of clear-sky reference. Selecting clear days as reference has two major flaws: (1) the profiles of temperature, humidity, and aerosol properties may change drastically enough to introduce a bias when assessing clear-cloudy changes in surface radiation budget components; (2) this method deviates from traditional model-based assessments that simply perform radiative transfer calculations with and without cloud condensate on the same vertical profiles. A perfect clear-sky estimate would produce zero change in net surface radiative fluxes where clouds are absent. However, looking at Fig. 5 (top, e.g., 5-6 and 18-19 UTC) the change is non-zero. Similarly, relations shown in Fig. 7-9 (middle) show non-zero change in surface budget components when the LWP approaches zero. These examples hint at an underlying bias of the analysis. In their revision, the authors need to repeat their analysis using a typical broadband radiative transfer code (e.g., RRTMG) to verify the change in net radiative fluxes.

→ This point is also a concern of the other reviewer, so we make a common response. We have performed, using several data sets, an in-depth study to evaluate the surface radiation components in clear-sky conditions.

#### 1) Supplementary data sets

In order to evaluate the surface radiation in clear-sky conditions at Concordia, we have used, in complement to BSRN observations, and at the closest location to Concordia station, two different data sets of surface radiations from:

a) the European Center for Medium-Range Weather Forecasts Reanalysis version 5 (**ERA5**). ERA5 is a climate reanalysis dataset, covering the period 1979 to present. ERA5 is being developed through the Copernicus Climate Change Service (C3S). Extracted data (<https://cds.climate.copernicus.eu/cdsapp#!/dataset/reanalysis-era5-single-levels>) used here are hourly at a regular horizontal grid of  $0.25^{\circ} \times 0.25^{\circ}$  in clear-sky conditions: surface solar and thermal infrared, downward and net radiations. As explained on the ERA5 website, clear-sky radiations are computed for the same atmospheric conditions of temperature, humidity, ozone, trace gases and aerosol as the corresponding total-sky quantities (clouds included), but assuming that the clouds are not there.

b) the Clouds and the Earth's Radiant Energy System (**CERES**), containing SYN1deg (Hourly CERES and geostationary (GEO) TOA fluxes, MODIS/VIIRS and GEO cloud properties, MODIS/VIIRS aerosols, and Fu-Liou radiative transfer surface and in-atmospheric (profile) fluxes consistent with the CERES observed TOA fluxes, as explained on <https://ceres.larc.nasa.gov/data/>). Surface fluxes in SYN1deg are computed with cloud properties derived from MODIS and geostationary satellites (GEO), where each geostationary satellite instrument is calibrated against MODIS (Doelling et al. 2013; 2016) at  $1^{\circ} \times 1^{\circ}$  horizontal resolution (<https://ceres.larc.nasa.gov/data/>). Aerosol and atmospheric data were included as inputs to calculate the radiation flux.

#### References:

[https://ceres.larc.nasa.gov/documents/DQ\\_summaries/CERES\\_SYN1deg\\_Ed4A\\_DQS.pdf](https://ceres.larc.nasa.gov/documents/DQ_summaries/CERES_SYN1deg_Ed4A_DQS.pdf)

Doelling, D. R., N. G. Loeb, D. F. Keyes, M. L. Nordeen, D. Morstad, C. Nguyen, B. A. Wielicki, D. F. Young, M. Sun, 2013: Geostationary Enhanced Temporal Interpolation for CERES Flux Products, *Journal of Atmospheric and Oceanic Technology*, **30**(6), 1072-1090. doi: [10.1175/JTECH-D-12-00136.1](https://doi.org/10.1175/JTECH-D-12-00136.1).

Doelling, D. R., M. Sun, L. T. Nguyen, M. L. Nordeen, C. O. Haney, D. F. Keyes, P. E. Mlynchak, 2016: Advances in Geostationary-Derived Longwave Fluxes for the CERES Synoptic (SYN1deg) Product, *Journal of Atmospheric and Oceanic Technology*, **33**(3), 503-521. doi: [10.1175/JTECH-D-15-0147.1](https://doi.org/10.1175/JTECH-D-15-0147.1).

#### 2) Comparison between ERA5, CERES and BSRN data.

We have compared the CERES and ERA5 data with the BSRN hourly-averaged data on the 5 reference days (clear-sky conditions) for the Net, LWD, LWU, SWD and SWU SRs. Figure R1 shows these variables for the 26 December 2021. The LWD and LWU values show an overall consistency between ERA5 and CERES (of the order of  $\sim 10 \text{ W m}^{-2}$ ), while a systematic negative bias of  $\sim 20\text{-}40 \text{ W m}^{-2}$  is observed with respect to BSRN data. However, the net longwave radiation, i.e. the difference  $\text{LWD} - \text{LWU}$  for each data set, is reduced to around  $5 \text{ W m}^{-2}$ . The SWD and SWU signals from ERA5, CERES and BSRN show a similar diurnal variation with differences less than  $50 \text{ W m}^{-2}$ . When considering the Net SR, some obvious differences up to  $50 \text{ W m}^{-2}$  can be seen between BSRN, ERA5 and CERES. Since the net longwave radiation is within  $10 \text{ W m}^{-2}$  for the three data sets, the source of this difference therefore should come from either SWD or SWU radiation.

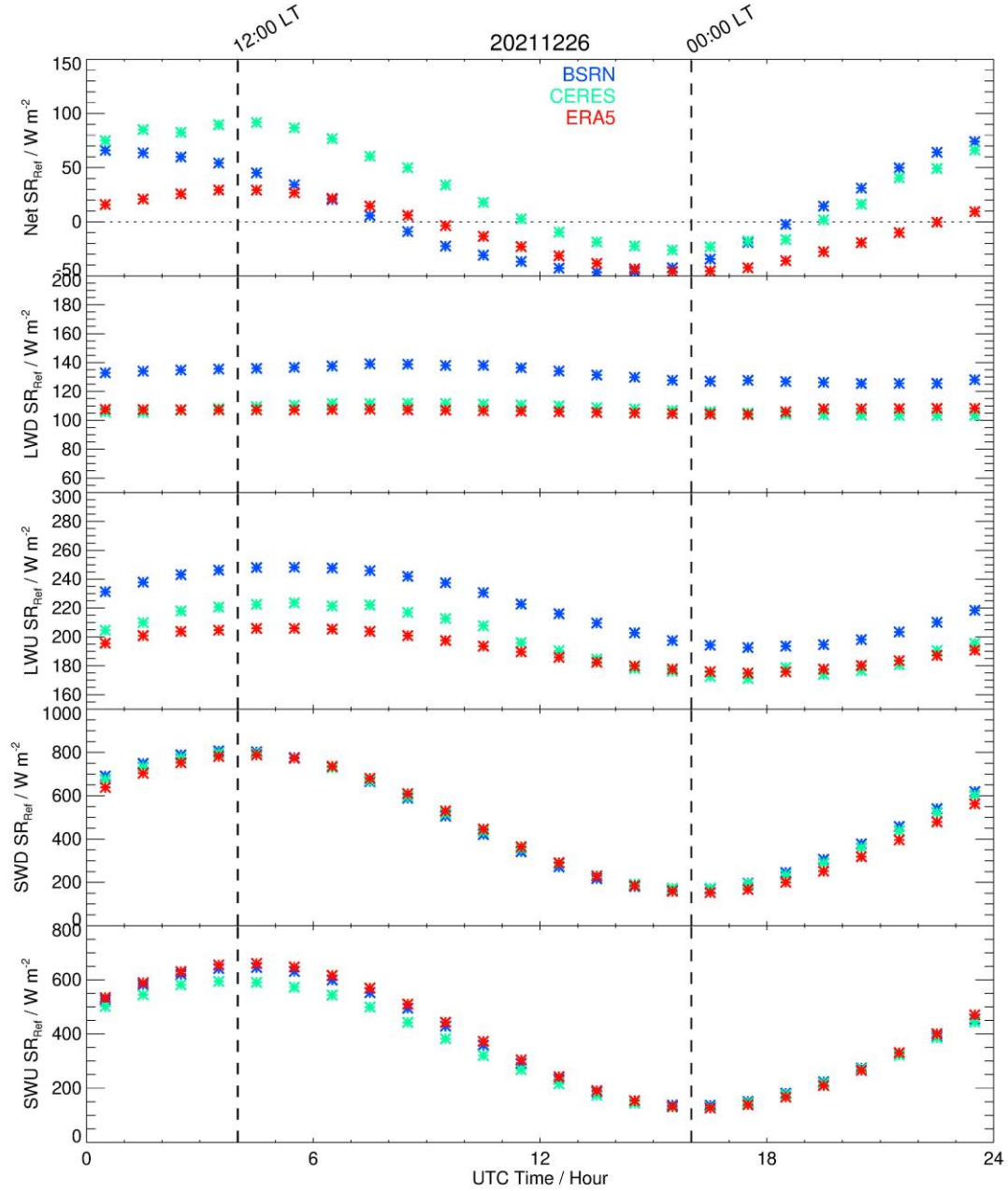


**Figure R1.** Hourly time evolution (UTC, hour) of the clear-sky surface radiations (SR,  $W m^{-2}$ ) observed by the BSRN instruments (blue asterisks), the CERES (green asterisks) and the ERA5 (red asterisks) data sets on 26 December 2021: (from top to bottom) Net SR, Longwave Downward (LWD SR), Longwave Upward (LWU SR), Shortwave Downward (SWD SR) and Shortwave Upward (SWU SR) surface radiations. The 00:00 and 12:00 local times (LT) are highlighted by 2 vertical dashed lines.

### 3) Impact of the local albedo on shortwave radiation.

We have calculated, for BSRN, ERA5 and CERES data, the albedo defined as:

$$\text{Albedo} = \text{SWU} / \text{SWD}.$$

Figure R2 shows the diurnal evolution of the albedo on 26 December 2021 (clear-sky day). The CERES and ERA5 albedos do not show any significant diurnal variation with quite constant

values of 0.74 and 0.83, respectively, whilst the observed BSRN albedo shows a clear diurnal signal with a maximum of 0.85 from 10:00 to 14:00 UTC (from 18:00 to 22:00 LT) and a minimum of 0.70 from 19:00 to 23:00 UTC (from 03:00 to 07:00 LT). The large diurnal signal present in the observed albedo is likely the signature of the sastrugi effect that is obviously absent in the ERA5 and CERES data sets. The BSRN SWU sensor has a circular footprint. For a sensor installed at a height  $h$  above the ground, 90% of the signal comes from an area at the surface closer than  $3.1 h$  (Kassianov et al., 2014). Since at Dome-C the instrument is installed at a height of 2-3 m, the albedo is thus determined by the surface elements in the immediate vicinity (a few meters) of the sensor.

Kassianov E, Barnard J, Flynn C, Riihimaki L, Michalsky J, Hodges G (2014) Areal-averaged spectral surface albedo from ground-based transmission data alone: toward an operational retrieval. *Atmosphere* 5:597–621. <https://doi.org/10.3390/atmos503059>

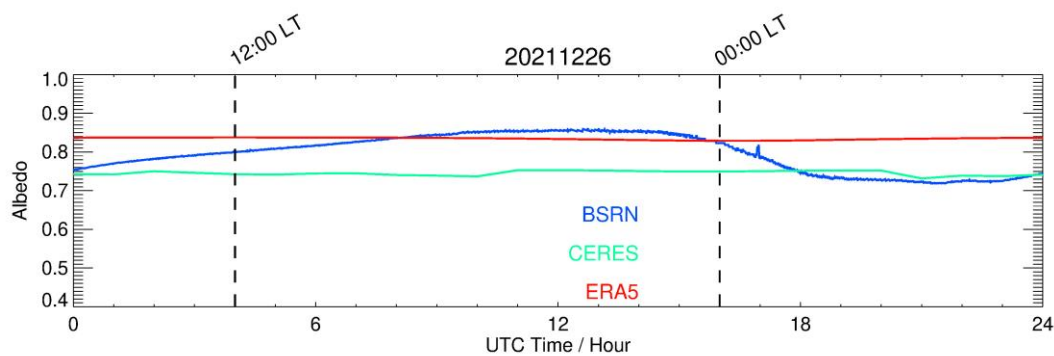


**Figure R2.** Time evolution (UTC, hour) of the surface albedo observed by the BSRN sensors (blue), the CERES (green) and the ERA5 (red) data sets on 26 December 2021. The 00:00 and 12:00 local times (LT) are highlighted by 2 vertical dashed lines.

#### 4) Impact of sastrugi on the albedo.

Sastrugi (Figure R3) are features formed by erosion of snow by wind. They are found in polar regions, and in snowy, wind-swept areas of temperate regions, such as frozen lakes or mountain ridges. Sastrugi are distinguished by upwind-facing points, resembling anvils, which move downwind as the surface erodes.



**Figure R3.** Image of sastrugi on the ice surface.



Figure R4 presents a satellite image showing the Concordia station. The sastrugi are clearly visible producing bright and dark straight lines with a 150°-330° orientation (wrt the N-S axis) (corresponding to solar azimuthal angles at ~13:00 and 01:00 LT). As a consequence, the albedo observed in BSRN is likely dependent of the sastrugi orientation, the sun elevation and the azimuthal angle.

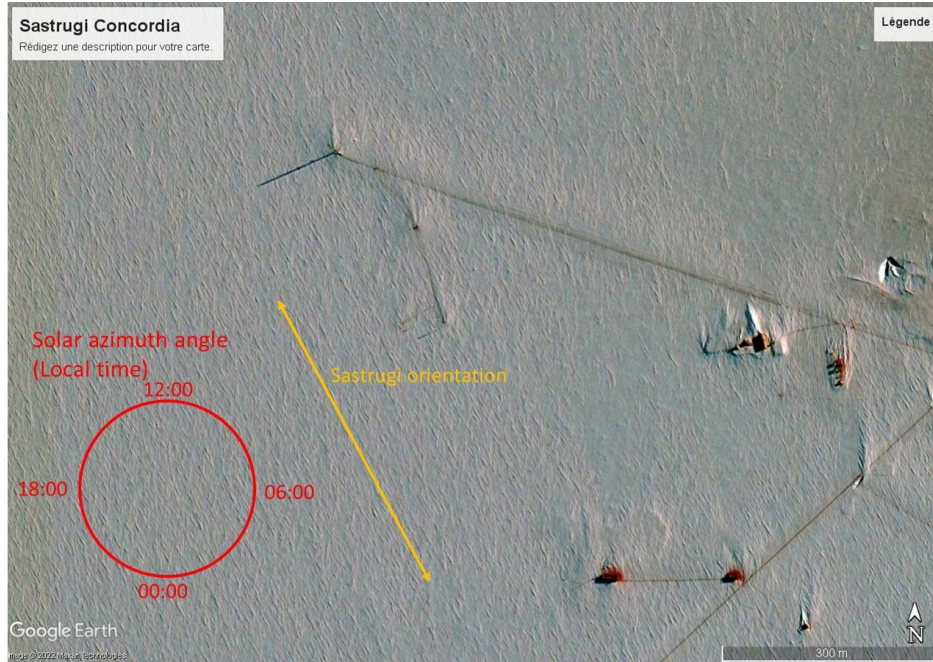


**Figure R4.** Images taken from Google Earth showing the Concordia station on the right-hand side. The sastrugi effect producing bright and dark straight lines is clearly visible with one main orientation at ~330° orientation (~11:00 local time solar azimuth angle, with 0° orientation towards the North).

If we suppose that the sastrugi effect impacts mostly SWU rather than SWD, and the albedo calculated from BSRN observations is the “truth”, we can calculate a modified SWU\* (including the sastrugi effect) for the ERA5 and CERES as:

$$\begin{aligned} \text{SWU(ERA5)}^* &= \text{SWD(ERA5)} \times \text{albedo(BSRN)} \\ \text{SWU(CERES)}^* &= \text{SWD(CERES)} \times \text{albedo(BSRN)} \end{aligned}$$

Then we calculate the modified Net SR\* (including the sastrugi effect) considering SWU\* for ERA5 and CERES. As an example, we present Figure R5, similar to Figure R1, in which we added the albedo, the SWU\* and Net SRs\* (including the sastrugi effect) for CERES and ERA5 (solid lines). We observe that the Net SR\* for ERA5 and CERES now coincides with the BSRN Net SR to within 5 W m<sup>-2</sup>, compared to differences up to 50 W m<sup>-2</sup> found when the sastrugi effect was not taken into account.

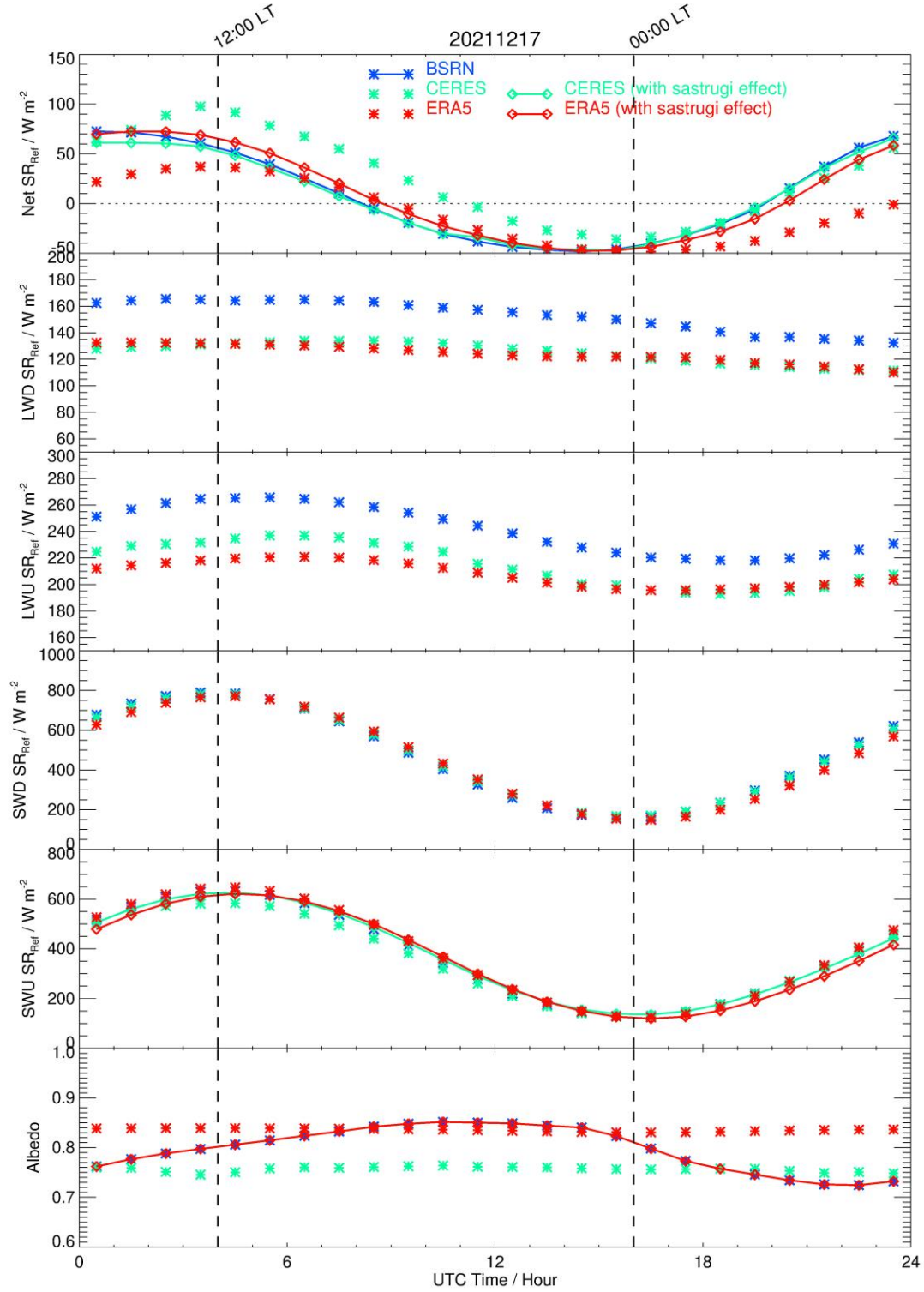


**Figure R5.** Same as Figure R1 with the albedo inserted in the lowermost panel. Net SR, SWU SR, and albedo including the sastrugi effect for ERA5 (red solid line) and CERES (green solid line) have also been added in the Figures.

We have fitted the BSRN albedo averaged over the 5 reference days with the sum of 2 sine functions, imposing periods of 24 and 12 hours. Figure R6 shows the BSRN albedo averaged over the five clear-sky days, the fitted trigonometric function and the residuals between the

averaged albedo and the fitted function. We can state that the sastrugi effect on the observed clear-sky albedo at Concordia is successfully fitted by 2 sine functions of 24h and 12h periods to within 0.003 mean absolute error, with a coefficient of determination  $R^2$  equal to 0.993 and a root mean square error of 0.0004.

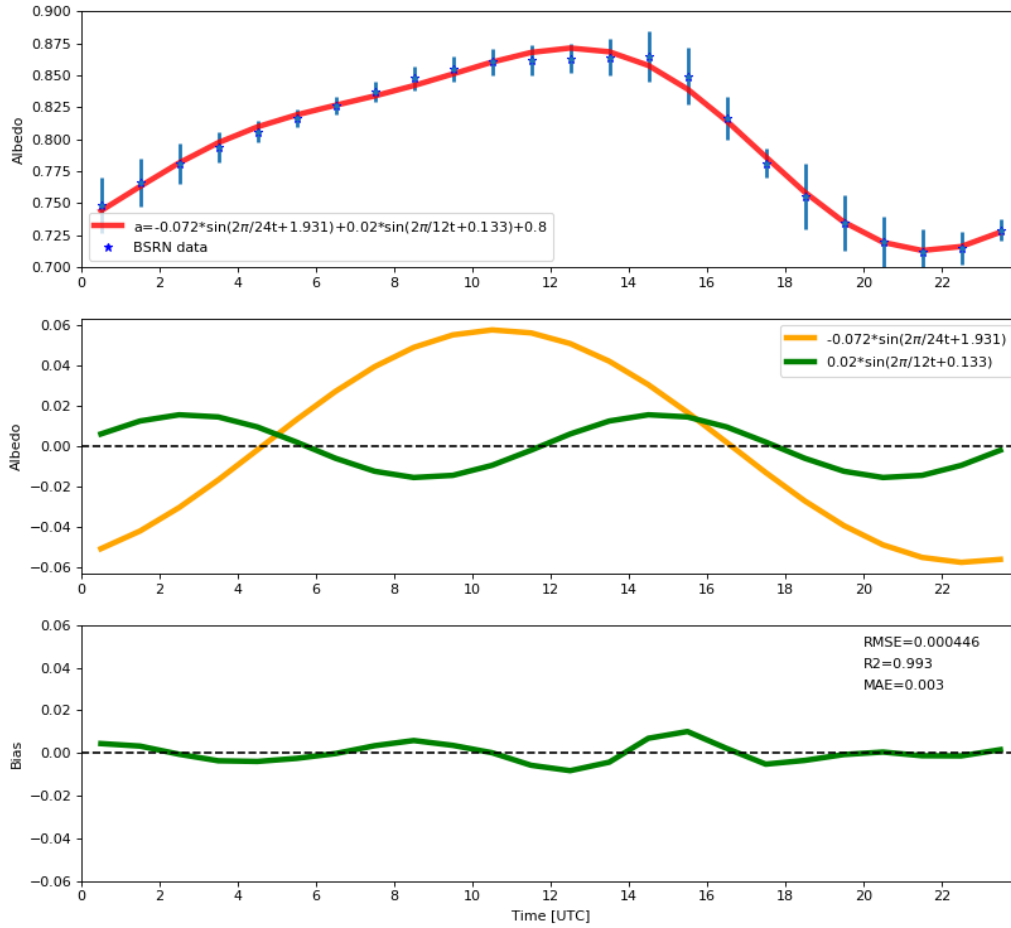


**Figure R6.** Top: Hourly time evolution (UTC, hour) of the mean surface albedo (blue stars) with the associated standard deviation (vertical bar) calculated from the BSRN data over the 5 clear-sky days together with the fitted trigonometric function made of two sine functions (red). Center: The two sine functions fitting the BSRN mean surface albedo. Bottom: bias of the fit curve (BSRN-fit) and associated root mean square error (RMSE), coefficient of determination ( $R^2$ ), and mean absolute error (MAE).

Moreover, we have considered all the BSRN observations in Decembers 2018, 2019, 2020 and 2021 to calculate the albedo (Figure R7), and we have superimposed the fitted trigonometric function as described in Figure R6. The presence of clouds is well highlighted by observations that depart from the fitted function whilst, during periods of clear-sky conditions, BSRN albedos coincide well with the fitted function.

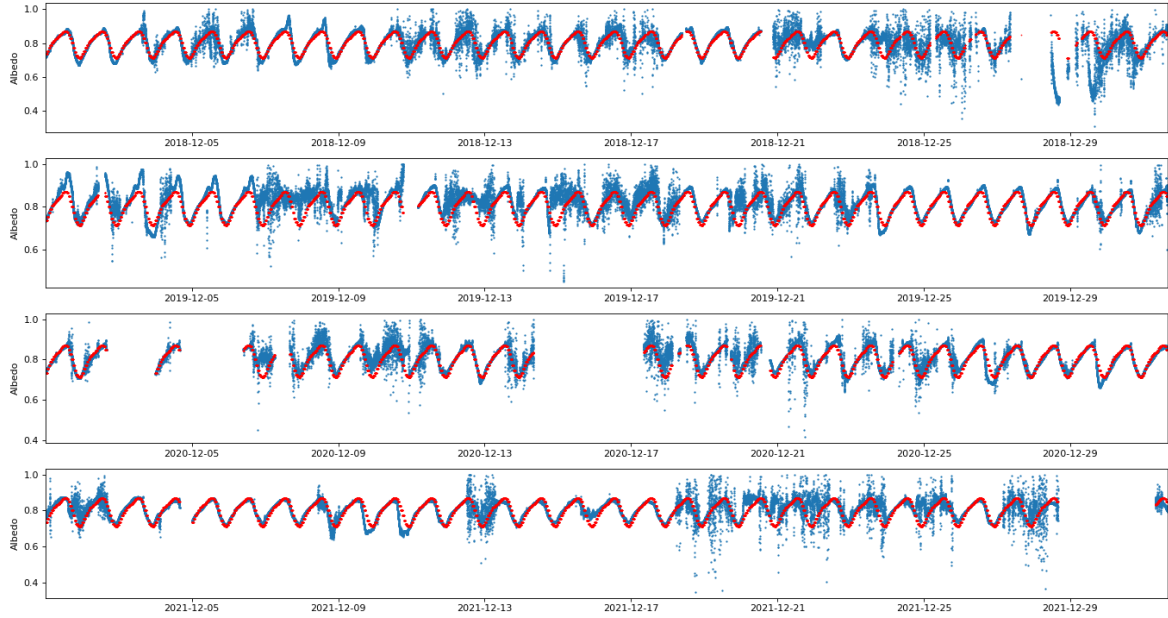


**Figure R7.** Hourly time evolution (UTC, hour) of the surface albedo observed by the BSRN instruments (blue), and the two-sine fit (red) for the whole BSRN data set covering the month of December in 2018, 2019, 2020 and 2021.

## 5) Conclusions

The study we have performed was extremely fruitful to evaluate the impact of the SLW clouds on the SR. The methodology requires reference clear-sky SR values that can be evaluated from: 1) models, 2) analyses and 3) observations. Our study has mainly shown that, at the Concordia station, sastrugi were present and strongly impacted the net SR via the surface albedo. This very local phenomenon cannot be taken into account by either the global-scale analyses (ERA5 and CERES), or standard radiative transfer models (e.g. RRTMG as suggested by the reviewers). As a consequence, the methodology we have developed based on field observations is likely the most powerful tool to estimate the Net SR in Concordia. It has some drawbacks, as for instance some biases for LWD and LWU between analyses and observations, but the LWD and LWU difference used to calculate the Net SR dramatically lessens the bias.

We have modified the revised version of the manuscript to explain the impact of the sastrugi effect on the SR by adding a detailed new section (see [sub-section 5.2](#)) and we have inserted a new paragraph in the [abstract](#) and in the [conclusion](#).



Looking at Figure 5 (top) the change in net radiative fluxes is strongly affected by spikes in upward and downward shortwave radiative fluxes. While the reason for these spikes may simply be rooted in three-dimensional radiative effects, it is unclear how these spikes affect the analysis. The authors should justify their current approach or else find a way to filter for homogenous conditions or smooth the measured shortwave fluxes.

→ We are not sure to properly understand the question of the reviewer. These spikes on the SR signals are not artifacts. They come from the inhomogeneity of the three-dimensional radiation received by the instrument. They are absent when: 1) clear-sky conditions are encountered, and 2) clouds broadly cover the sky. Such spikes appear mainly 1) during scattered conditions and 2) when large cloud episodes appear or disappear. They are not restricted to the Concordia conditions but may appear at any latitude. For example, considering a similar instrumentation installed at the University of Toulouse, France, Figure R8 shows the time evolution of the SWD SR in clear-sky and cloudy conditions, together with the difference of the two (cloudy minus clear-sky signals). Negative as well as positive spikes appear in the difference when clouds are present likely due to incoming radiation reflected on cloud surface. Therefore, at Concordia, these spikes may also come from the inhomogeneity of the cloud distribution. As a conclusion, we do not consider that despiking is required because our approach is based on real field observations.

We mention this point in the revised manuscript (end of **sub-section 3.1**).

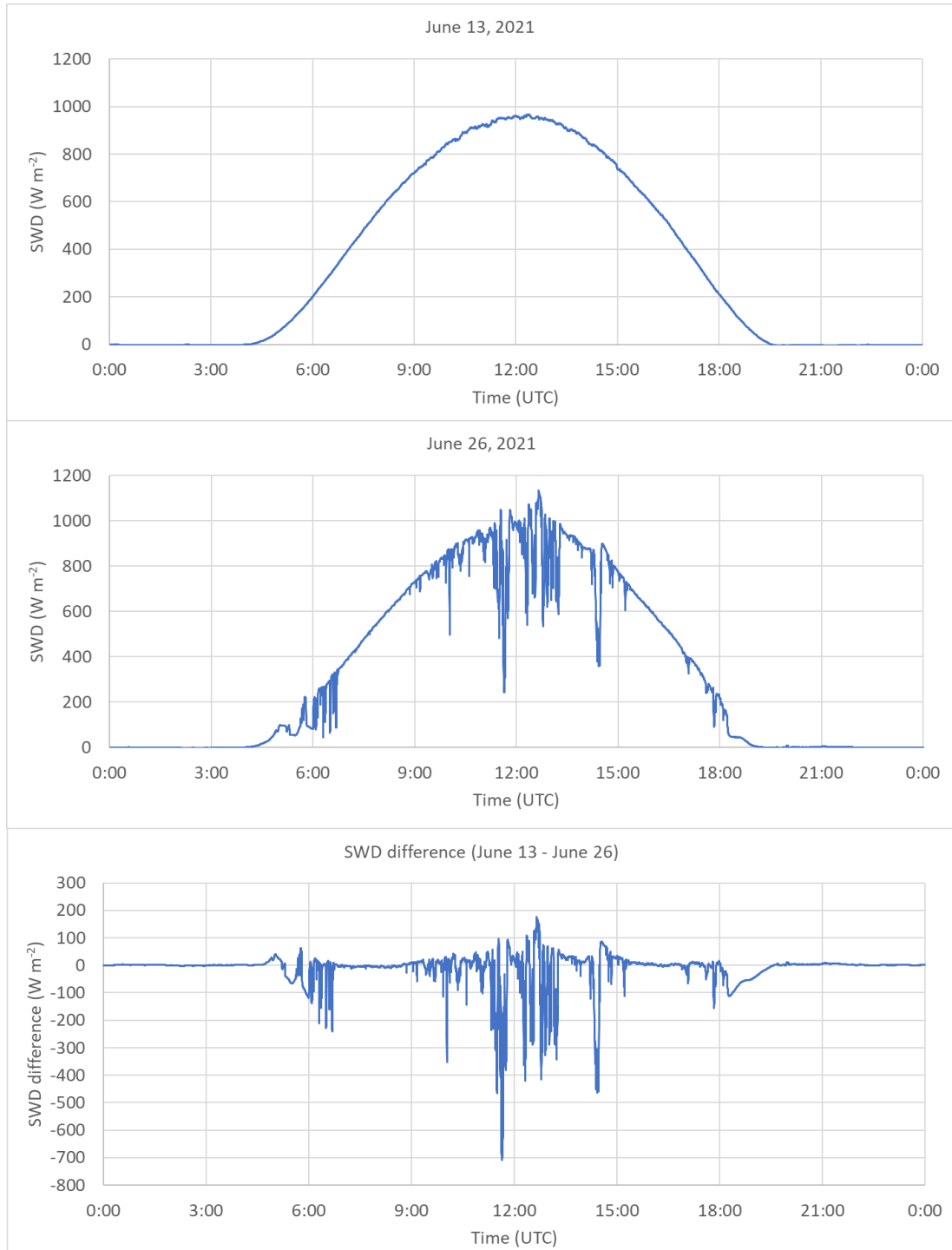


**Figure R8.** Time evolution of the shortwave downward surface radiation ( $\text{W m}^{-2}$ ) observed in Toulouse (France) in clear-sky conditions on 13 June 2021 (top), in cloudy conditions on 26 June 2021 (middle) and difference between the two (bottom). Data time sampling is 10 sec.

The article contains numerous instances of vague or non-scientific language that confuse when reading. For example, the authors refer to “liquid water concentration” (l. 79) which should probably be “liquid water content”. Instead of listing a measurement of “radiation” (l. 92), the authors need to be more specific (i.e., “radiative flux” or “irradiance”). Measuring “aerosol and clouds” (l. 112) leaves a lot of room for speculation and needs to be specified. “Temperature” is a key metric and it is unclear whether the authors used potential temperature of liquid-water

potential temperature. The latter one is a conserved variable in a well-mixed, cloudy boundary layer and should be used. Using the former one (as maybe done here) would introduce a systematic error into the analysis that affect a key finding (i.e., a LWP-temperature relationship). The authors need to clarify which temperature was used and also over which altitudes the temperature was averaged (I'm guessing it is the cloud layer?).

→ We carefully checked the manuscript to avoid any confusion in terminology. We clarify below some points highlighted by the reviewer:

- We changed “liquid water concentration” into “liquid water content” as suggested.
- Our use of the term “radiation” is consistent with the terminology presented page 256 of Stull (1988). We have inserted the following sentence and reference in the revised manuscript.

Hereafter, we will use either the term “radiative flux” or “radiation”, the latter consistent with the terminology presented page 256 by Stull (1988).

Stull, R. B.: An introduction to boundary layer meteorology. Kluwer Academic Publisher, 1988.

- We have used the regular temperature within the SLW cloud. We clarified this in the revised paper.
- (l. 112): we changed the incriminated text for “cloud characteristics” and we detail in the following paragraphs (see [sub-section 2.1](#)) of the manuscript which parameters are actually retrieved by the Lidar instrument.

Looking at Figure 1, there appears to be frozen precipitation below some clouds (e.g., 7-8 and 18:30 – 19:30 UTC) as indicated by relatively great backscatter and depolarization ratio. It is unclear how (any) precipitation affects the HAMSTRAD liquid water content (or path) retrieval; the authors need to explain this. Furthermore, frozen precipitation hints at frozen particle inside clouds; the authors should discuss this issue and ideally refine their identification of supercooled clouds to ensure ice-free conditions.

→ Microwave observations at 60 and 183 GHz are not sensitive to ice crystals. This has already been discussed in Ricaud et al. (2018) when considering the study of diamond dust in Antarctica. As a consequence, precipitation detected by the Lidar does not affect retrievals of temperature, water vapour and liquid water. Nevertheless, during long episodes of large precipitation that can happen in winter periods, some amount of snow can accumulate on the shield protecting the HAMSTRAD radiometer. In summer time, a technician looks after the instrument and sweeps out the accumulated snow. But in winter, it is much more difficult for a technician to move outside of the base and unfortunately the sweeping may be performed few days after an intensive period of precipitation. As a consequence, snow that accumulates on the HAMSTRAD protective shield can perturb the 183-GHz signal, thus water vapour and LWP retrievals. But we recall that our present analysis is performed for the summer months of December 2018-2021 when precipitation is less intense and manpower very active to look after the instrument. We have added some sentences in the revised manuscript to clarify the issue of precipitation and impact on the LWP retrievals (see at the end of [sub-section 2.2](#)).

Another point is the ice-free conditions of the cloud we analyze. As mentioned in the text, we cannot state that the SLW clouds we study are 100% constituted of liquid water. Because of the methodology employed based on the depolarization ratio, the SLW clouds we observed are obviously made of liquid water. But there might be some periods when, associated with the SLW cloud, an ice layer is also detected above the SLW layer. We agree that this solid water layer may, at some stage, diffuse and/or precipitate within the SLW layer. The cloud in its whole might be formed of an ice layer superposed to a SLW layer. Unfortunately, in our present study, we cannot go through this macroscopic process by only using remote-sensed observations. In the discussion section 5.5 “Other clouds”, these points were already presented.

### Minor concerns

II.. 53-54 While hydrometeors are larger, does the total water path change (or does it stay constant)? Please report.

→ This point has been dealt just above. Furthermore, hydrometeors are found to be larger on the coast than over the continent so the impact of the hydrometeors on LWP retrievals is even lower at Concordia than on the coast.

II. 55-60 This sentence is too long and lacks clarity. For example, what object is referred to in “two to three times lower...”.

→ The incriminated sentence has been changed into the Introduction as:

Based on the raDAR/liDAR-MASK (DARDAR) spaceborne products (Listowski et al., 2019), it has been found that clouds are mainly constituted of ice above the continent. The abundance of Supercooled Liquid Water (SLW, the water staying in liquid phase below 0°C) clouds depends on temperature and liquid/ice fraction. It decreases sharply poleward, and is two to three times lower over the Eastern Antarctic Plateau than over the Western Antarctic.

II. 68-69 This sentence makes is sound like supercooled water emerges from heterogenous nucleation. Please rephrase.

→ We rewrote the sentence into the Introduction as:

Liquid water in clouds may occur in supercooled form due to a relative lack of ice nuclei for temperature greater than -39°C and less than 0°C.

I. 72 Please find an appropriate reference (perhaps within Storelvmo and Tan, 2015?).

→ We have added the 3 historical references in the revised manuscript and modified the sentences in the Introduction accordingly.

Very little SLW is then expected because the ice crystals that form in this temperature range will grow at the expense of liquid droplets (called the “Wegener-Bergeron-Findeisen” process; Wegener, 1911; Bergeron, 1928; Findeisen, 1938; Storelvmo and Tan, 2015).



Bergeron, T., 1928: Über die dreidimensional verknüpfende Wetteranalyse. – Geophys. Norv.

Findeisen, W., 1938: Kolloid-meteorologische Vorgänge bei Niederschlagsbildung. Meteorol. Z. 55, 121-133. (translated and edited by Volken, E., A.M. Giesche, S. Brönnimann. – Meteorol. Z. 24 (2015), DOI:10.1127/metz/2015/0675).

Wegener, A. 1911. Thermodynamik der Atmosphäre. – Leipzig, Germany: Barth.

I. 92 Please change “radiation” to “radiative flux”.

→ Done

I. 112 Please specify “aerosol and clouds”. Which properties were retrieved?

→ To be more focused on cloud characteristics, which is the main topic of the paper, we prefer not to detail Lidar capabilities for observing aerosols. We thus modified the term “aerosol and clouds” that is too vague into “cloud characteristics”. The Lidar cloud observations are detailed farther in the manuscript (see sub-section 2.1).

I. 149 Please add “radiative” before “fluxes”.

→ Done

II. 191-192 This sentence needs rephrasing to improve readability.

→ We have modified the sentence into (sub-section 3.1):

Since it is impossible to measure for the same day the SR with and without cloud, we have in priority looked for clear-sky days over the months of December in the 2018-2021 period.

II. 266-268 I’m assuming liquid-water potential temperature was used (i.e., a conserved variable in a cloudy boundary layer). Also, could these warm events also be moist – in other words, are there perhaps warm-moist intrusions that explain this LWP-temperature relation?

→ No, as explained in our response to a comment above and in the revised manuscript, we have not used liquid-water potential temperature but regular temperature.

Episodes of warm-moist intrusions exist above Concordia originated from mid-latitudes (Ricaud et al., 2017 and 2020) and known as “atmospheric rivers” (Wille et al., 2022). Although they are infrequent, they may provide high values of temperature and LWP. We have inserted a new sentence and a new reference associated to this point (see sub-section 4.1).

Wille, J.D., Favier, V., Dufour, A., Gorodetskaya, I.V., Turner, J., Agosta, C. and Codron, F., 2019. West Antarctic

surface melt triggered by atmospheric rivers. *Nature Geoscience*, 12(11), pp.911-916.

II. 300-302 This sentence contains too many verbs. Perhaps remove “is”.

→ We modified the incriminated sentence and moved the corresponding paragraph to **sub-section 5.1**.

II. 382-385 Not sure what “This” refers to. Please rephrase.

→ We have rephrased the sentence in the revised sub-section 5.5:

As a consequence, the presence of mixed-phase clouds in addition to SLWCs may explain the negative part of the Net, LWD and LWU  $\Delta SR$  ( $[-20;0]$   $W m^{-2}$ ) and the positive part of the SWD and SWU  $\Delta SR$  ( $[0;10]$   $W m^{-2}$ ) for low values of LWP ( $[0.8;1.6]$   $g m^{-2}$ ).

II. 444-445 The link doesn't work. Please check.

→ We changed the link to “9news” since the link to “LA Times” did not work all the times:

<https://www.9news.com.au/world/antarctica-heatwave-extreme-warm-weather-recorded-concordia-research-station/3364dd91-2051-4df5-8cfc-5f2819058604>

Section 5.1 – The authors start a line of thinking that seems unfinished. I suggest the authors either flesh this out and compute whether a change in temperature truly explains the change in LWP or else shift the focus of this subsection to discuss the influence if warm-moist intrusions (as suggested above) or other meteorological drivers.

→ We have moved this section as a note in the **new 5.2 section “Reference Surface Radiation and sastrugi effect”**.

Section 5.5 – To make this rough estimate believable the authors should report whether LWPs in other Antarctic regions are comparable.

→ The horizontal distribution and the temporal evolution of LWP over Antarctica is presented in Lenaerts et al. (2017) based on 2007-2010 reanalyses, observations and climate models. Over Antarctica, LWP is on average less than  $10 g m^{-2}$ , with slightly larger values in summer than in winter by  $2-5 g m^{-2}$ . Over the Western Antarctica, LWPs are larger ( $20-40 g m^{-2}$ ) than over the Eastern Antarctica ( $0-10 g m^{-2}$ ). As a consequence, LWP observed at Concordia is consistent with values observed over the Eastern Plateau, with a factor 2-4 smaller than those observed over the Western continent. We have inserted a new paragraph and a new reference in the revised **section 5.6**.

Lenaerts, J.T., Van Tricht, K., Lhermitte, S. and L'Ecuyer, T.S., 2017. Polar clouds and radiation in satellite observations, reanalyses, and climate models. *Geophysical Research Letters*, 44(7), pp.3355-3364.

Figure 1 - Please improve the lower end of the color scale for depolarization ratio (i.e., near 5% that is used as threshold).

→ We have modified the Figure accordingly (see Figure R9 below).

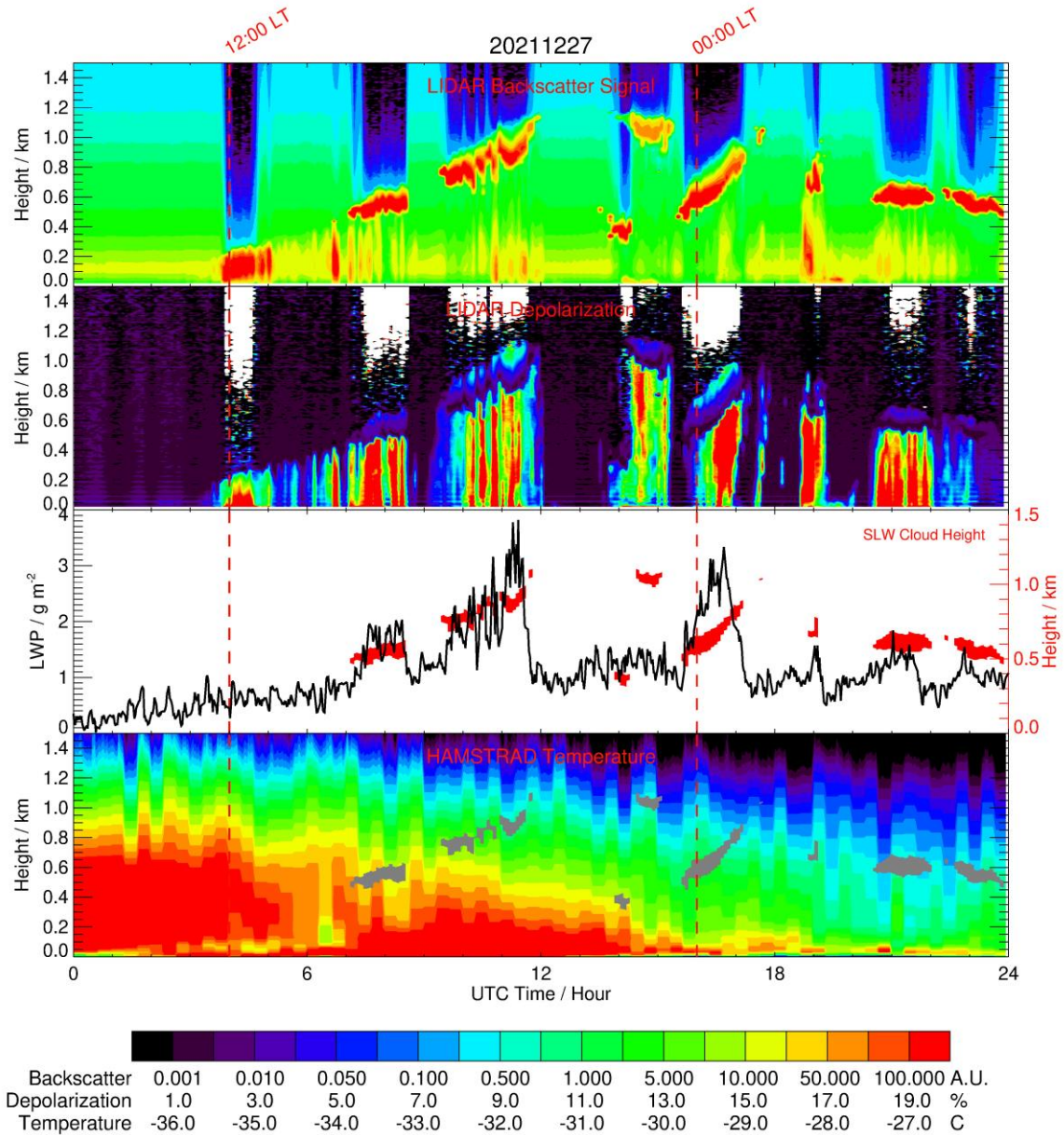


Figure R9: (From top to bottom): Time evolution (UTC, hour) of the Lidar Backscattering Signal, the Lidar Depolarization Signal, the HAMSTRAD LWP and the HAMSTRAD temperature profile measured on 27 December 2021. The time evolution of the SLW cloud (as diagnosed by a backscattering signal  $> 60$  A.U. and a depolarization signal  $< 5\%$ ) is highlighted by the red and grey areas in the third and the forth panel from the top, respectively. The height above the ground is shown on the third panel from the top with the y-axis on the right. The 00:00 and 12:00 local times (LT) are highlighted by 2 vertical dashed lines.

Figure 2 – The detailed images should be shown at higher quality to enable a visual assessment of the presence of ice-cloud features (e.g., halo). Also an image should be shown for the period 4-5 UTC that was brought up in the main text.

→ The images come from an automated camera and this is the highest quality we can have. The point is that we show only 2 sets of images: 1) cloud-free and 2) SLWCs. We do not show any ice cloud so it is not expected to visualize any halo.

Unfortunately, the camera stopped acquiring images between 03:47:16 and 05:35:11 UTC. So we cannot insert any other image for this period in Figure 2.

Figure 6 – It is unclear which temperature is shown (absolute, potential, or liquid-water potential temperature) and which layers were used for averaging (e.g., in-cloud layers only?).

→ This point is dealt above. We clarified the methodology employed. We show regular temperature. There is no averaging at all. The Lidar profiles are interpolated along the temperature vertical grid and then according to the temperature time sampling. As a consequence, for a given time and height, we have a depolarization ratio, a backscatter signal, a regular temperature and a (not height-dependent) LWP. The same method is used for SR. BSRN SRs are time interpolated to be coincident with the LWP values. As a consequence, for a given time, we have a set of BSRN SRs (Net, LWU, LWD, SWU and SWD) and an LWP. At a (time, height) point showing high backscatter signal and low depolarization, the associated parameters (regular temperature, LWP and SRs) are flagged as “SLW cloud”. The statistic is thus done using all the SLW-flagged points without any averaging. The temperature corresponds to the in-cloud temperature.

The text has been modified accordingly (see sub-section 3.1)

Figure 6-9 – It is unclear why the authors decided to determine statistics (i.e., the bars) in horizontal direction. Isn't the question for example in Figure 7 “which change in net radiative budget corresponds to a certain LWP” which would call for a statistic per LWP (i.e., producing a vertical bar)?

→ We agree that it could have been interesting to make the analysis in the way suggested by the reviewer. However, we wanted to study the sensitivity of LWP for a given temperature and for a given radiation component (Net, LWD, LWU, SWD, SWU). We inserted a sentence in the revised manuscript (see sub-section 3.2).

This study is focused on the evaluation of the LWP sensitivity for a given temperature and for a given radiation component (Net, LWD, LWU, SWD, SWU).